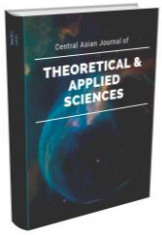

CENTRAL ASIAN JOURNAL OF THEORETICAL AND APPLIED SCIENCE

https://cajotas.centralasianstudies.org/index.php/CAJOTAS

Volume: 06 Issue: 03 | July 2025 ISSN: 2660-5317

Article

DFT Study of the Properties of Monolayer and Bilayer Hexagonal InN Nanosheets Compared to the Wurtzite Phase

Ali Y. Abd Alrhman[1], Issa Z. Hassan*[2], Abdulkarim Ziedan Khalf[3]

1,2,3. Department of Physics, College of Education for Pure Sciences, University of Kirkuk, Kirkuk, Iraq
*Correspondence: i.hassan@uokirkuk.edu.iq

Abstract: Due to the wide range of potential applications for III-nitride nanostructures in nanodevices, this study aimed to investigate the structural, optical, and electronic properties of bulk Wurtzite indium nitride (InN) compared to those of two-dimensional monolayer and bilayer structures using Density Functional Theory (DFT). The study found that the energy gap for bulk Indium Nitride was 0.076 eV when using the GGA-PBE exchange-correlation functional, while it was 0.85 eV when the hybrid functional (HSE03) was used, indicating a direct energy gap. As the thickness of the material decreased to the monolayer InN, the energy gap increased to 0.402 eV with the GGA-PBE functional and 1.354eV with the hybrid functional (HSE03) and the energy gap increased to 0.729 eV with the GGA-PBE functional and 1.801 eV with the hybrid functional (HSE03), transitioning to an indirect type. This is attributed to the higher accuracy of the hybrid functional (HSE03) compared to the GGA-PBE functional. Overall, the findings demonstrate that the energy gap increases as the thickness of InN decreases, transitioning from direct to indirect bandgap. Additionally, a shift in the absorption spectrum from infrared to ultraviolet radiation is observed. Consequently, it can be concluded that the energy gap of InN can be tuned and controlled by adjusting the material's thickness, depending on the requirements of the desired application.

Keywords: DFT, InN, Monolayer, Electronic Band Structure, Optical Properties, Hybrid Functional

Citation: Alrhman, A. Y. A., Hassan, I. Z., Khalf, A. Z. DFT Study of the Properties of Monolayer and Bilayer Hexagonal InN Nanosheets Compared to the Wurtzite Phase. Central Asian Journal of Theoretical and Applied Science 2025, 6(3), 263-274.

Received: 30th Apr 2025
Revised: 10th May 2025
Accepted: 17th May 2025
Published: 26th May 2025

1. Introduction

Nanomaterials are considered one of the most important pillars of science and technology in the 21st century. Their remarkable properties stem from the reduction of material size to the nanoscale (between 1 and 100 nanometers). Beyond this size, the physical, chemical, mechanical, and electronic properties of the material deviate greatly from its behavior in the typical bulk state [1]. This is due to quantum confinement effects, increased surface area to volume ratio and dominance of grain boundaries, which are key factors in the overall free energy of the material. Nanomaterials include nanoparticles, nanotubes, nanowires and nanoporous materials, each of which has unique properties suitable for specific applications.

Nanomaterials are regarded as one of the key foundations of science and technology in the 21st century. Their extraordinary characteristics arise from reducing materials to the nanoscale, measuring between 1 and 100 nanometers. At this scale, the physical, chemical, mechanical, and electronic attributes of a material significantly differ from its behavior in the conventional bulk state [1]. This phenomenon is attributed to quantum confinement effects, a higher surface area to volume ratio, and the prominence of grain boundaries, all of which are crucial factors influencing the overall free energy of the material.

Nanomaterials encompass nanoparticles, nanotubes, nanowires, and nanoporous substances, each possessing distinct properties tailored for specific uses.

Recently, nanomaterials with hexagonal honeycomb structures (from carbon nanotubes to two-dimensional (2D) materials such as graphene, hexagonal boron and monolayer chalcogenides) have attracted much attention due to their properties that can be used in various nanodevices [2,3]. Among these materials, group III nitride nanostructures exhibit unusual properties not observed in other 2D hexagonal materials [4]. These materials can have flat or curved structures, with monolayer indium nitride (InN) being one of the flat structures in this group [4]. The physical properties of layered materials are very sensitive to external influences such as deformation or external fields [5-7]. Most ultrathin 2D nanomaterials are obtained from large multilayer crystals using top-down and bottom-up approaches. These materials exhibit weak interlayer van der Waals interactions and strong intralayer covalent bonds. 2D materials are widely used in electronics, optoelectronics [8,9], gas sensing [10-14], energy storage [15,16], and chemical catalysis [17,18] due to their unique physical, mechanical, and chemical properties that can be controlled by thickness. The narrow bandgap of InN (0.7 eV), strong absorption, and data transmission capabilities make it essential for high-efficiency solar cells [19,20] and high-speed electronic systems [21,22]. Density Functional Theory (DFT) first-principles calculations were carried out in this study utilising the CASTEP software package. . The study focused on two models of pure indium nitride (InN): monolayer InN and bulk InN of the wurtzite phase. The study emphasized understanding the electronic and optical properties, comparing the results, and identifying the differences between them to determine the best outcomes that can be utilized in various applications based on the material's properties.

Recently, nanomaterials featuring hexagonal honeycomb structures—ranging from carbon nanotubes to two-dimensional (2D) materials like graphene, hexagonal boron, and monolayer chalcogenides—have garnered significant interest due to their potential applications in a variety of nanodevices. Among these materials, group III nitride nanostructures showcase unique properties that are not found in other 2D hexagonal materials. These structures can be either flat or curved. Monolayer indium nitride (InN) represents one of the flat variants. The physical characteristics of layered materials are highly responsive to external factors such as deformation and external fields. Most ultrathin 2D nanomaterials are derived from larger multilayer crystals through top-down or bottom-up synthesis methods. These materials demonstrate weak van der Waals forces between layers while maintaining strong covalent bonds within layers. Due to their distinctive physical, mechanical, and chemical traits, which can be adjusted based on thickness, 2D materials are extensively utilized in fields such as electronics, optoelectronics, gas sensing, energy storage, and chemical catalysis. The narrow bandgap of InN (0.7 eV), along with its excellent absorption and data transmission capabilities, makes it crucial for the development of high-efficiency solar cells and advanced high-speed electronic systems. This study employed Density Functional Theory (DFT) first-principles calculations using the CASTEP software package, focusing on two models of pure indium nitride: monolayer InN and bulk InN in the wurtzite phase. The research aimed to explore the electronic and optical properties, compare the findings, and highlight the differences between the two models to ascertain the most beneficial applications based on the material's characteristics.

2. Materials and Methods

Density Functional Theory (DFT) first-principles calculations were carried out in this study, utilizing the Cambridge Series Total Energy Package (CASTEP) software. A specific type of exchange-correlation energy was used in the current study [23]. Calculations were conducted on three models of pure indium nitride (InN): the first model was a large supercell (3x3x1) for the hexagonal monolayer InN, the second model was a large supercell

(3x3x**1**) for the bilayer InN, and the third model was a large supercell (3x3x3) for the bulk InN in the wurtzite phase. The calculations were carried out after completing the geometry optimization as the first step to obtain electronic properties such as the energy gap and determining whether it is direct or indirect, as well as the total and partial density of states. The GGA-PBE approximation was also used to compute optical characteristics, including the dielectric constant, absorption coefficient, and reflection. For the energy gap, the HSE03 approximation was used exclusively.

3. Results and Discussion

From this study, we concluded the electronic structure to determine the energy gap, as well as the total and partial density of states. The optical properties for each type were then analyzed and compared.

3.1 Structural Properties

Hexagonal indium nitride (InN) consists of two atoms, nitrogen and indium, which are bonded together to form hexagonal cells resembling a honeycomb structure. The bond length between the indium (In) and nitrogen (N) atoms for the bulk InN model is 3.586 Å, with the lattice constants being $a = b = 3.614123$ Å and $c = 5.835$ Å, as shown in Figure 1a.

The lattice constants for the bilayer InN model are $a = b = 3.73$ Å and $c = 80.774$ Å, while the bond length between the atoms is 2.149 Å. Figure (1b) shows that the distance between the two layers is 2.565 Å and the angle between the three atoms is 119.976°.

The lattice constants in the monolayer InN model are $a = b = 3.614$ Å and $c = 23.75685$ Å, while the bond length between the atoms is 2.087 Å. Figure 1c illustrates the 120° angle that exists between the three atoms. Following the completion of the supercell's geometry optimization procedure, these values were theoretically acquired by computer simulations [24].

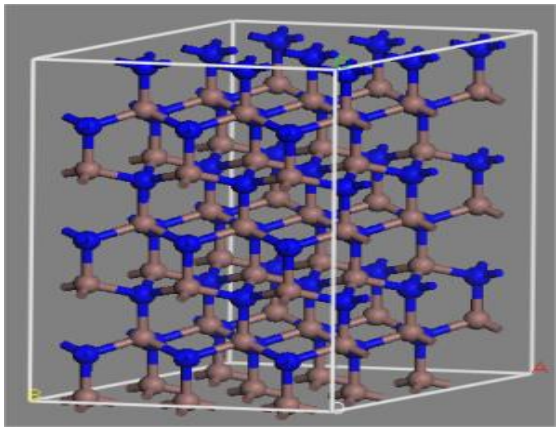

Figure (1a). Bulk indium nitride InN .

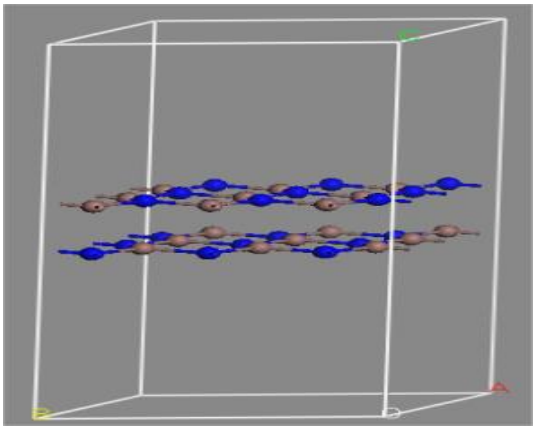

Figure (1b). Bilayer indium nitride InN.

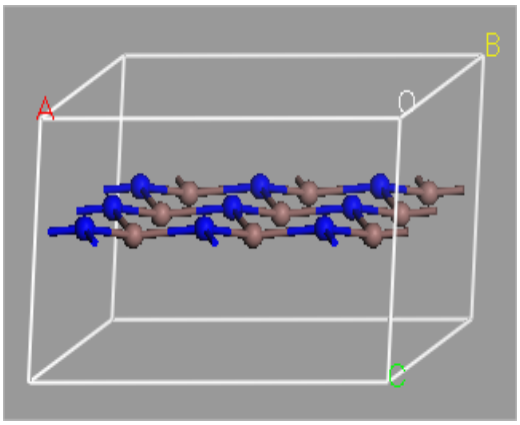

Figure (1c). Monolayer indium nitride InN.

3.2 Electronic Properties

The energy bands and electron distribution in the crystal structure determine the basic electronic and optical properties of the material. Starting from the band structures of three forms of indium nitride (InN), their electronic properties can be analyzed using the (GGA) and (HSE03) functions determined by density functional theory (DFT) calculations.

The direct band gap of the InN wurtzite phase was determined to be 0.85 eV using the HSE03 function (see Figure 2b) and 0.076 eV using the GGA function (see Figure 2a). Figure 2c shows the partial and total density of states of the direct band gap type. This shows that in the crystal space, the maximum of the valence band and the minimum of the conduction band are located on the same wave vector. This straight band gap is crucial for the suitability of the material for optical and electrical applications because it enables efficient radiative transitions.

As shown in Figure 3a, the indirect band gap of bilayer InN is determined to be 0.402 eV using the GGA function, and 1.354 eV using the HSE03 function (see Figure 3b). Figure 3c shows the partial and total density of states for the indirect band gap type.

As shown in Figure 4a, the indirect band gap of monolayer InN is determined to be 0.729 eV using the GGA function, and 1.801 eV using the HSE03 function (see Figure 4b). Figure 4c displays the partial and total density of states for the indirect band gap type. Table 1 compares and presents the results for bulk indium nitride, Table 2 compares the results for bilayer indium nitride, and Table 3 compares the results for monolayer indium nitride. From these results, it is evident that the energy gap increases and the type of gap transitions from direct to indirect as the material transitions from bulk indium nitride to monolayer indium nitride. Thus, we can control the energy gap and adjust it to the desired value to suit specific applications.

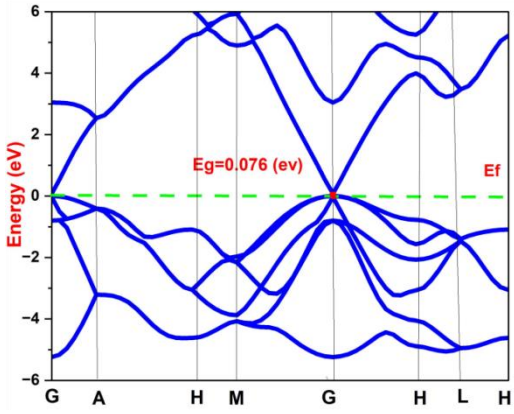

Figure (2a). Bulk indium nitride InN using the GGA. energy gap.

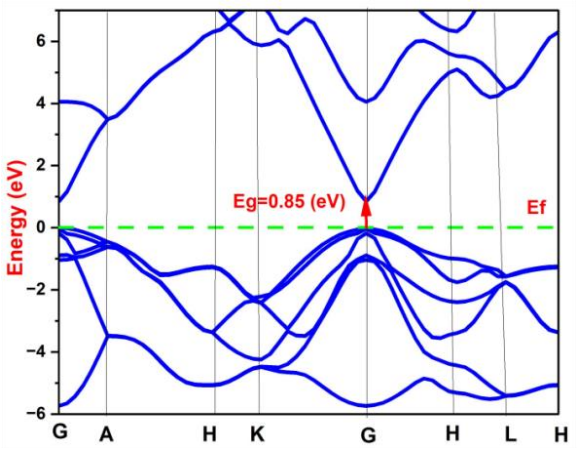

Figure (2b). Energy gap bulk indium nitride InN using the HSE03.

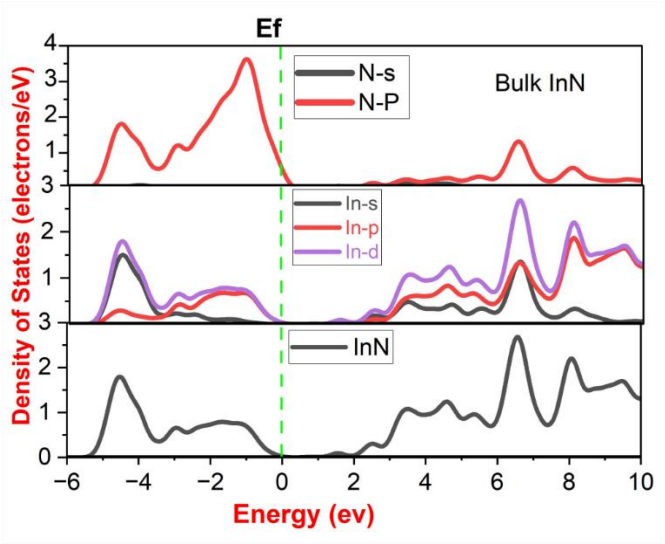

Figure (2c). Partial and total density of states bulk indium nitride InN.

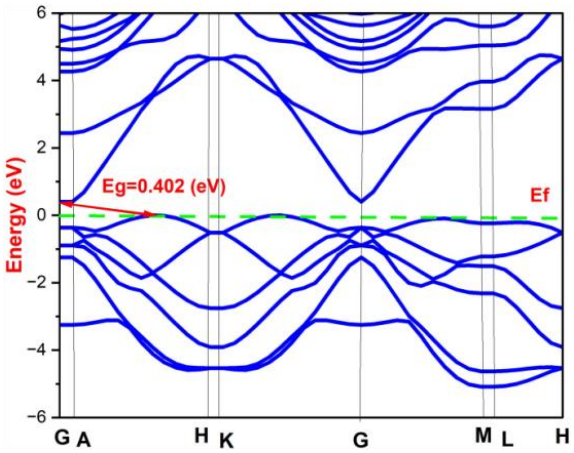

Figure (3a). Bilayer indium nitride InN using the GGA . energy gap.

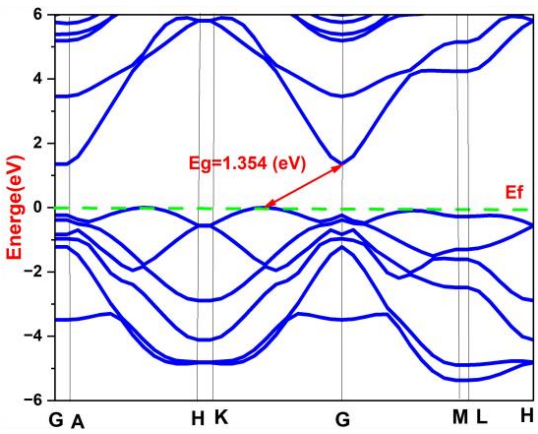

Figure (3b). Energy gap bilayer indium nitride InN using the HSE03.

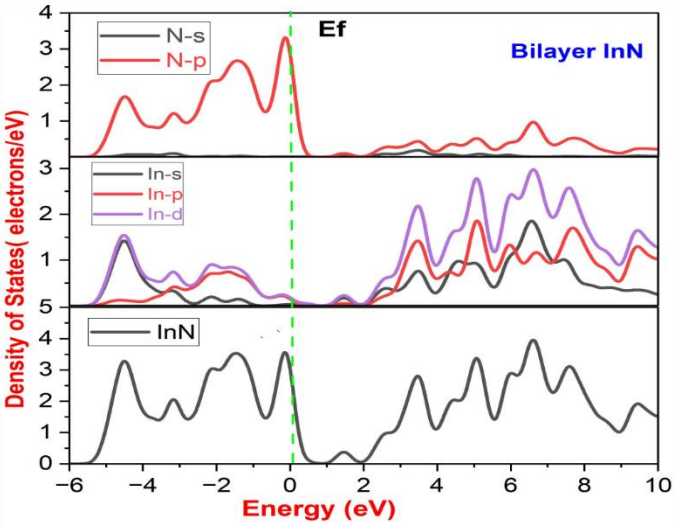

Figure (3c). Partial and total density of states bilayer indium nitride InN.

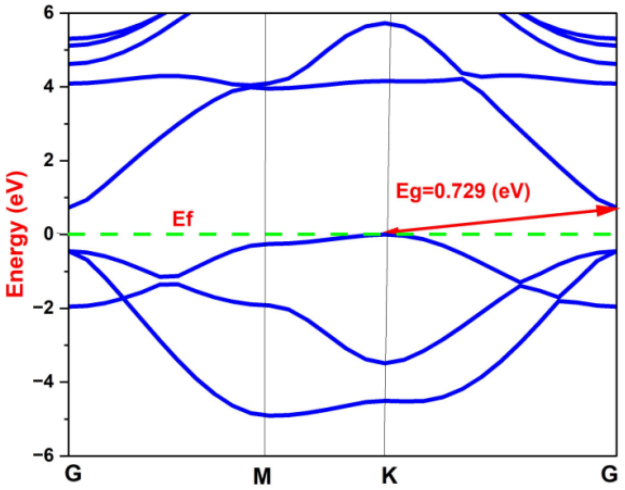

Figure (4a). Energy gap monolayer indium nitride InN using the GGA.

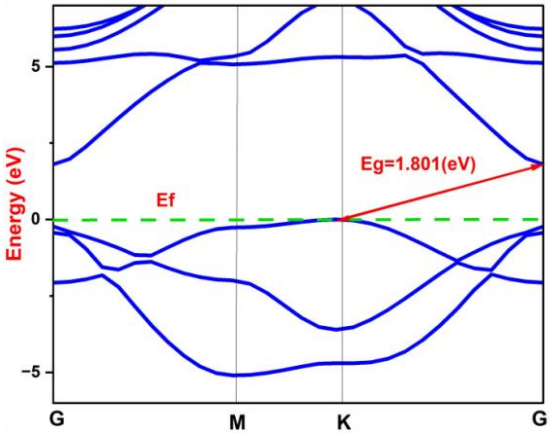

Figure (4b). Energy gap monolayer indium nitride InN using the HSE03.

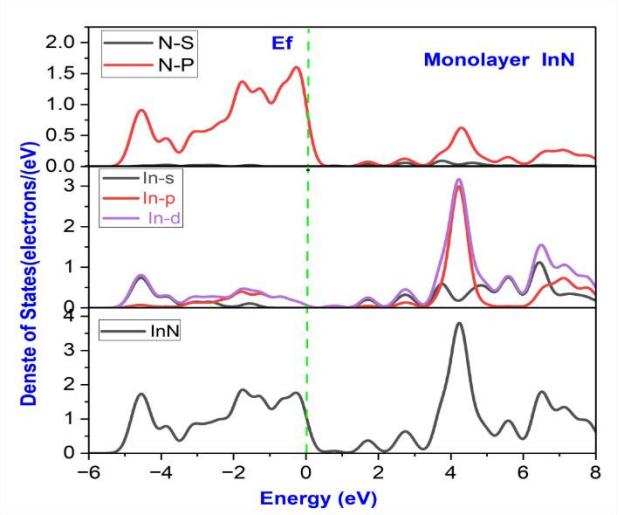

Figure (4c). Partial and total density of states monolayer indium nitride InN.

Table 1. Lattice constants a=b and c, bond length d, and band gap Eg. Calculated for bulk InN using PBE and HSE03 methods.

Buik InN	**a=b (Å)**	**c (Å)**	**d (In-N) (Å)**	**Eg(eV)**	Previous studies **(eV)**
GGA	3.612586	5.835053	3.586	0.076	[25]/(0.37) [26]/(0.029)
HSE03	3.612586	5.835053	3.586	0.85	[27-31]/(0.78-0.90)

Table 2. Lattice constants a = b and c, bond length d, and Energy band gap Eg, calculated using the PBE and HSE03 approaches for bilayer InN.

Bilayer InN	**a=b (Å)**	**c (Å)**	**d (In-N)(Å)**	**Eg(eV)**	**Previous studies Eg(eV)**
GGA	3.37	80.774	2.149	0.402	[32]/ 0.33
HSE03	3.37	80.774	2.149	1.354	----------

Table 3. Lattice constants a=b and c, bond lengths d, and energy bands given as Eg. Calculated using PBE and HSE03 methods for hexagonal monolayer InN.

Monolayer InN	a=b (Å)	c (Å)	d (In-N)(Å)	Eg(eV)	Previous studies Eg(eV)
GGA	3.614123	23.75685	2.087	0.729	[33]/ 0.712
HSE03	3.614123	23.75685	2.087	1.801	[34]/ 2±0.1

3.3 Optical Properties

The optical properties were studied using the General Gradient Approximation (GGA) for the wurtzite phase of bulk indium nitride and for the hexagonal bilayer and monolayer indium nitride, and the corresponding plots for each model were obtained.

For bulk indium nitride, Figure (5a) represents the relationship between frequency and absorption coefficient. The absorption region extends from 0 eV to 31.297 eV, with the highest absorption value of 311267.805 cm^{-1} occurring at the point 10.077 eV. Figure (5b) shows the relationship between frequency and reflection. Figure (5c) represents the relationship between frequency and both the real and imaginary dielectric constants.

For bilayer indium nitride, Figure 6a shows the relationship between frequency and absorption coefficient, where the absorption region extends from 0 eV to 21.378 eV, with the highest absorption peak of 25404.190 cm^{1} at 8.810 eV. Figure (6b) represents the relationship between frequency and reflection. Figure (6c) shows the relationship between frequency and the real and imaginary dielectric constants.

For monolayer indium nitride, Figure 7a represents the relationship between frequency and absorption coefficient, where the absorption region extends from 0 eV to 20.754 eV, with the highest absorption peak of 47075.444 cm^{1} at 9.159 eV. Figure (7b) shows the relationship between frequency and reflection. Figure (7c) represents the relationship between frequency and both the real and imaginary dielectric constants.

It can be concluded that bulk indium nitride, due to its small band gap, has the capacity to absorb light from deep infrared radiation. As the thickness of the material decreases and approaches a monolayer, the band gap increases, causing its light absorption capabilities to shift from the infrared region to the visible and ultraviolet regions.

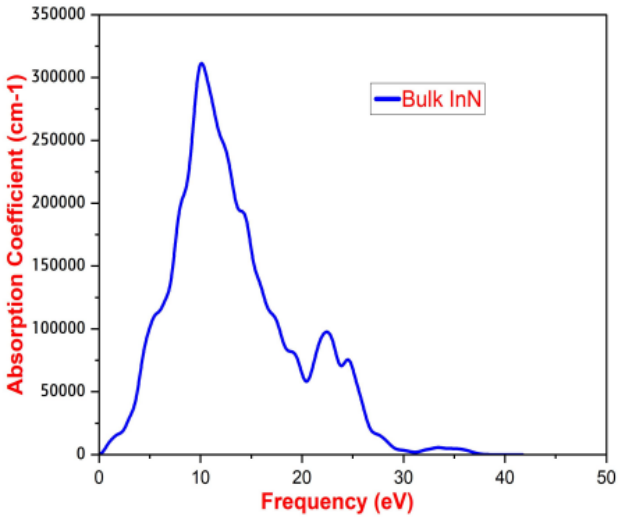

Figure (5a). The relationship between frequency and absorption coefficient bulk indium nitride.

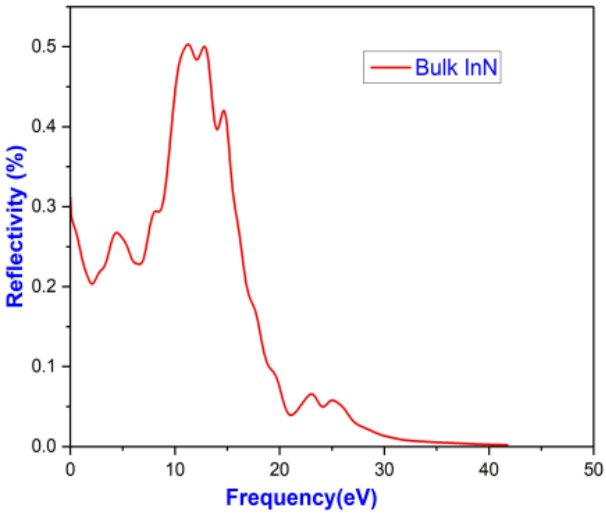

Figure (5b). The relationship between frequency and reflection bulk indium nitride.

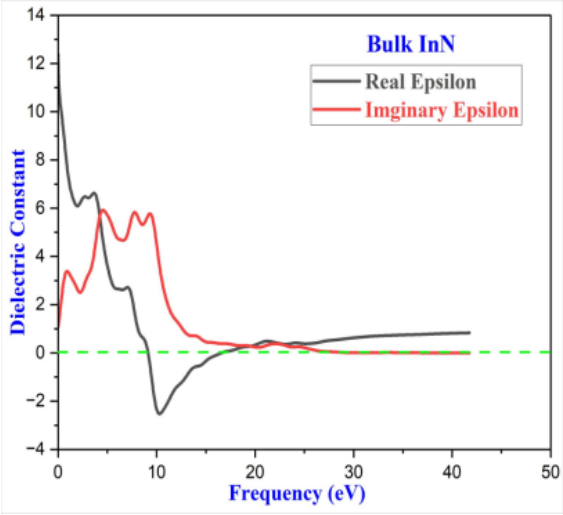

Figure (5c). The relationship between frequency and both the real and imaginary dielectric constants bulk indium nitride.

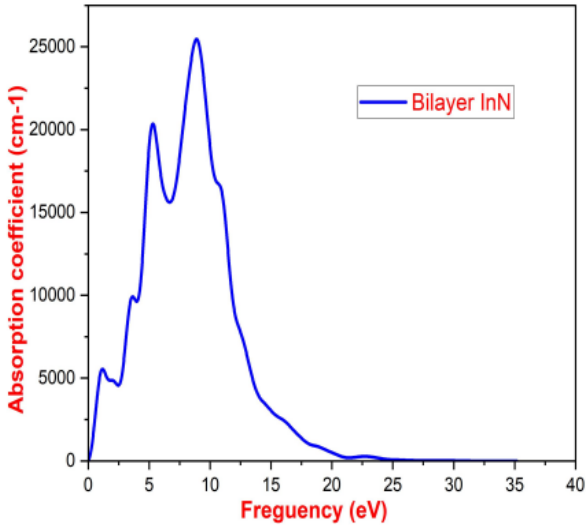

Figure (6a). The relationship between frequency and absorption coefficient bilayer indium nitride.

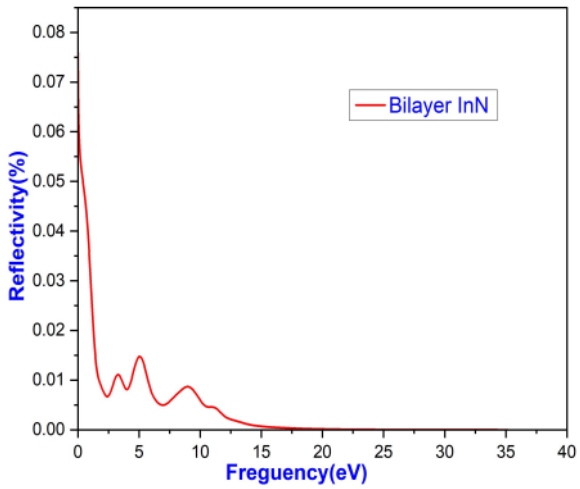

Figure (6b). the relationship between frequency and reflection bilayer indium nitride.

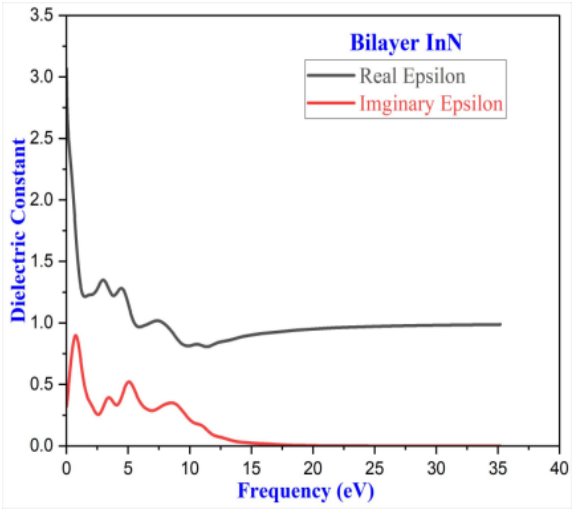

Figure (6c). The relationship between frequency and both the real and imaginary dielectric constants bilayer indium nitride.

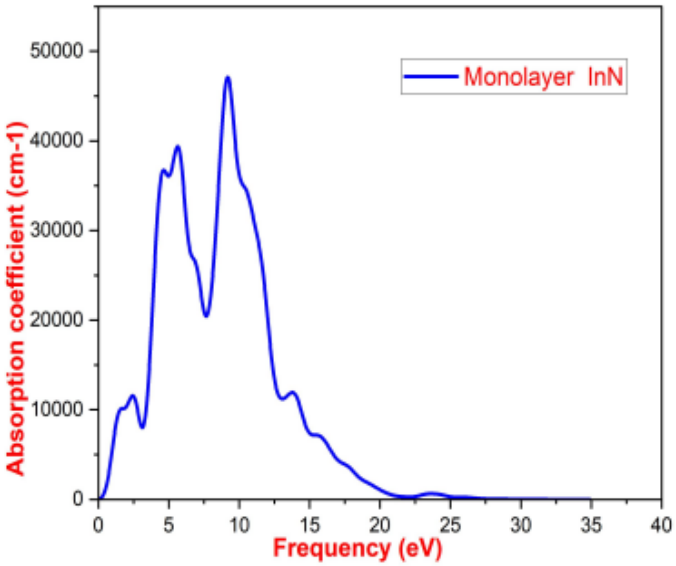

Figure (7a). The relationship between frequency and absorption coefficient monolayer indium nitride.

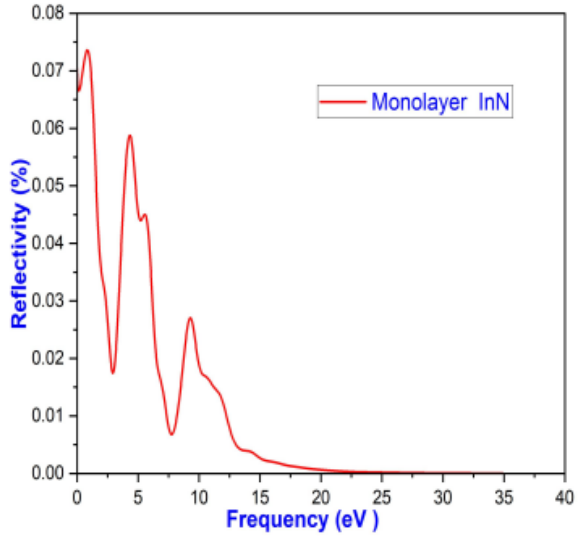

Figure (7b). The relationship between frequency and reflection monolayer indium nitride.

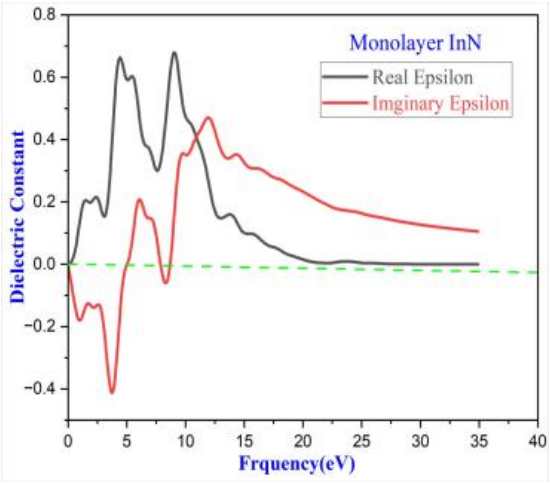

Figure (7c). The relationship between frequency and both the real and imaginary dielectric constants monolayer indium nitride.

4. Conclusion

We studied the structural, electronic and optical properties of indium nitride (wurtzite phase). as well as hexagonal bilayer and monolayer indium nitride, using Density Functional Theory (DFT). The results obtained indicate that the energy gap increases and transitions from a direct type to an indirect type when the material changes from bulk to bilayer and monolayer phases, as concluded from both the GGA and HSE03 approximations. This suggests that as the thickness of indium nitride decreases, its electronic and optical properties change. For instance, the absorption spectrum of monolayer and bilayer indium nitride shifts towards the blue spectrum compared to bulk InN. This feature offers significant potential for applications in optoelectronics due to its tunable band gaps.

REFERENCES

[1]R. Kumar, G. Mariappan, and A. Ashok Kumar, "Nano Fiber and Nano Particles for Various Functional Product developments," 2022.

[2]K. S. Novoselov, D. Jiang, F. Schedin, T. J. Booth, V. V. Khotkevich, S. V. Morozov and A. K. Geim, Proc. Natl. Acad. Sci. U. S. A., vol. 102, pp. 10451, 2005.

[3]M. Yarmohammadi, RSC Adv., vol. 7, pp. 10650, 2017.
[4]H. Şahin, S. Cahangirov, M. Topsakal, E. Bekaroglu, E. Akturk, R. T. Senger and S. Ciraci, Phys. Rev. B: Condens. Matter Mater. Phys., vol. 80, p. 155453, 2009.
[5]P. T. T. Le, M. Davoudiniya and M. Yarmohammadi, Phys. Chem. Chem. Phys., vol. 21, p. 238, 2019.
[6]M. Yarmohammadi, J. Magn. Magn. Mater., vol. 426, pp. 621, 2017.
[7]M. Yarmohammadi, AIP Adv., vol. 6, p. 085008, 2016.
[8]J. Shim, H.-Y. Park, D.-H. Kang, J.-O. Kim, S.-H. Jo, Y. Park and J.-H. Park, Adv. Electron. Mater., vol. 3, no. 4, p. 1600364, 2017.
[9]Q. A. Vu and W. J. Yu, J. Korean Phys. Soc., vol. 73, pp. 1–15, 2018.
[10]G. R. H. Abdullah and I. Z. Hassan, "A computational study of the properties of pure, adsorbed, and doped zinc oxide with copper and nickel atoms," Central Asian Journal of Theoretical and Applied Science, vol. 5, no. 6, pp. 592–603, 2024.
[11]S. S. Varghese, S. H. Varghese, S. Swaminathan, K. K. Singh and V. Mittal, Electronics, vol. 4, no. 3, pp. 651–687, 2015.
[12]S. Zhai, X. Jiang, D. Wu, L. Chen, Y. Su, H. Cui and F. Wu, Surf. Interfaces, vol. 37, p. 102735, 2023.
[13]H. Wu, Y. Xia, C. Zhang, S. Xie, S. Wu and H. Cui, Mol. Phys., vol. 121, no. 3, p. e2163715, 2023.
[14]Z. Nie, C. Wang, R. Xue, G. Xie and H. Xiong, Appl. Surf. Sci., vol. 608, p. 155119, 2023.
[15]H. M. Awad and I. Z. Hassan, "A Computational Study of the Effect of Adsorbed Nickel on the Hydrogen Storage Capacity in the Solid State on the Surface of Molybdenum Disulfide," Central Asian Journal of Theoretical and Applied Science, vol. 5, no. 6, pp. 555–562, 2024.
[16]B. Mendoza-Sánchez and Y. Gogotsi, Adv. Mater., vol. 28, no. 29, pp. 6104–6135, 2016.
[17]D. Deng, K. Novoselov, Q. Fu, N. Zheng, Z. Tian and X. Bao, Nat. Nanotechnol., vol. 11, no. 3, pp. 218–230, 2016.
[18]J. Di, C. Yan, A. D. Handoko, Z. W. Seh, H. Li and Z. Liu, Mater. Today, vol. 21, no. 7, pp. 749–770, 2018.
[19]A. Yamamoto, M. Tsujino, M. Ohkubo and A. Hashimoto, Sol. Energy Mater. Sol. Cells, vol. 35, pp. 53–60, 1994.
[20]A. Yamamoto, M. R. Islam, T.-T. Kang and A. Hashimoto, Phys. Status Solidi C, vol. 7, no. 5, pp. 1309–1316, 2010.
[21]S. Zhao, B. Le, D. Liu, X. Liu, M. Kibria, T. Szkopek, H. Guo and Z. Mi, Nano Lett., vol. 13, no. 11, pp. 5509–5513, 2013.
[22]A. G. Bhuiyan, A. Hashimoto and A. Yamamoto, J. Appl. Phys., vol. 94, no. 5, pp. 2779–2802, 2003.
[23]R. Ahmed and I. Hassan, "Study of the electronic properties of pure nanostructured hexagonal Zinc Oxide by DFT method," Al-Kitab Journal for Pure Sciences, vol. 7, no. 2, pp. 78–88, Oct. 2023.
[24]H. Schlegel, "Geometry optimization," vol. 1, no. 5, pp. 790–809, 2011.
[25]C. Stampfl and C. G. Van de Walle, Phys. Rev. B, vol. 59, pp. 5521–5535, 1999.
[26]R. Graine, R. Chemam, F. Z. Gasmi, R. Nouri, H. Meradji and Khenata, Int. J. Mod. Phys. B, vol. 29, p. 1550028, 2015.
[27]K. Kim, W. R. Lambrecht and B. Segall, Phys. Rev. B, vol. 53, pp. 16310, 1996.
[28]B. Paulus, F. H. Shi and H. Stoll, J. Phys.: Condens. Matter, vol. 9, pp. 2745–2758, 1997.
[29]J. H. Edgar, *Properties of Group-III Nitrides*, EMIS Datareviews Series, IEE, London, 1994.
[30]P. Carrier and S. H. Wei, J. Appl. Phys., vol. 97, p. 033707, 2005.
[31]J. Wu, et al., Appl. Phys. Lett., vol. 80, pp. 3967–3969, 2002.
[32]V. Wang, Z. Q. Wu, Y. Kawazoe and W. T. Geng, J. Phys. Chem. C, 2018.
[33]T. V. Vu et al., RSC Adv., vol. 10, no. 18, pp. 10731–10739, 2020.
[34]B. Pécz, G. Nicotra, F. Giannazzo, R. Yakimova, A. Koos, and A. Kakanakova-Georgieva, Adv. Mater., vol. 33, no. 1, p. e2006660, 2021